



Trade Science Inc.

# Organic CHEMISTRY

An Indian Journal

Full Paper

OCAIJ, 8(2), 2012 [46-51]

## Tautomerization of 4-(2-thiazolylazo) resorcinol: A DFT study

Ali Beyramabadi\*, Ali Morsali

Department of Chemistry, Mashhad Branch, Islamic Azad University, Mashhad, (IRAN)

E-mail: beiramabadi6285@mshdiau.ac.ir

Received: 9<sup>th</sup> May, 2011 ; Accepted: 9<sup>th</sup> June, 2011

### ABSTRACT

The 4-(2-Thiazolylazo) resorcinol (TAR) ligand could exist as two enol-imino (**E**) and keto-enamine (**K**) tautomers. In this work, the structural parameters, energetic content, natural bond orbital analysis, as well as tautomerization mechanism of the **E** and **K** tautomers of the TAR are investigated, employing density functional theory and the PCM model. Also, the percentage of tautomers and activation energy of the tautomerization reaction are computed in the gas phase and methanol solution. Both of the tautomers have a planar structure. In the gas phase, the **E** form is more stable, whereas the **K** tautomer is dominant by considering the solvent effects. The tautomerization reaction includes an intramolecular-proton transfer. © 2012 Trade Science Inc. - INDIA

### KEYWORDS

Azo compound;  
4-(2-Thiazolylazo) resorcinol;  
Enol-keto tautomerism;  
Density functional theory;  
PCM;  
Intramolecular proton transfer.

### INTRODUCTION

Azo compounds and their complexes of great importance because of their interest thermal and optical properties and applications in optical data storage, photoswitching, non-linear optics and photochromic materials, dyes, chemical analysis and pharmaceuticals<sup>[1-5]</sup>. Also, from a biological point of view, they show a range of biological activities such as carcinogenesis, antibacterial and inhibitor of DNA, RNA, and protein synthesis<sup>[6,7]</sup>.

4-(2-Thiazolylazo) resorcinol (TAR) is a well-known chelating reagent in spectrophotometric determination of metal ions<sup>[8,9]</sup>, separation of trace metal ions of the food and environmental samples<sup>[10,11]</sup> and acid-base titrations as an indicator<sup>[12,13]</sup>. Also, many metal complexes of the TAR have been synthesized<sup>[9,10,14-17]</sup>.

Now, theoretical investigations have much applica-

bility in many areas of the chemistry, such as kinetics and mechanism investigations of the reactions, spectroscopic assignments, characterization of the molecular structures, and so on<sup>[18-24]</sup>. They could, at the same time, be considered as complementary to or replacement for experimental methods.

In this work, we have theoretically investigated the geometrical structures and energy contents of the TAR conformers, as well as the mechanism of tautomerization reaction in the gas and solution phases. In addition, the natural bond orbital (NBO), atomic charges and the frontier molecular orbital (FMO) analysis were performed.

### THEORETICAL METHODS

All DFT calculations have been performed with the Gaussian 98 software package<sup>[25]</sup> by using the B3LYP

hybrid functional<sup>[26]</sup> and the 6-311+G(d,p) basis set. First, all degrees of freedom for all geometries were optimized. The optimized geometries were confirmed to have no imaginary frequency of the Hessian. The frequency calculations were performed at the same computational level to evaluation of the zero-point energies and the Gibbs free energies.

Here, the Polarizable Continuum Model (PCM)<sup>[27]</sup> has been employed for investigation of solute-solvent interactions. The gas phase optimized geometries were used to apply the solvent effects in methanol as solvent.

## RESULTS AND DISCUSSION

### Geometry optimization

In this work, geometries of the **E** and **K** conformers of the TAR have been fully optimized in the gas phase. Some of the calculated structural parameters are gathered in TABLE 1. The calculated structural parameters are in good agreement with the corresponding values reported for similar compounds<sup>[9,10,14-17]</sup>.

Another conformer is also possible for each of the **K** and **E** tautomers, in which the thiazolyl ring rotates around the C9-N2 bond, so that position of the S1 atom is changed with the N3 atom. In these structures, all three nitrogen atoms of the ligand (N1, N2 and N3) are roughly in the same direction. Our calculations shown that these new structures are unstable. During the optimization process, the input structure converts to the **E** (or **K**) tautomer by rotation of the thiazolyl ring around the C9-N2 bond. Therefore, there are only two stable conformers for the TAR, **K** and **E**, which are investigated in below.

The optimized geometries of the **K** and **E** tautomers of the TAR ligand are shown in Figure 1. The calculated dihedral angles such as C6-N1-N2-C9 and C3-C6-N3-S1 demonstrate that both the **E** and **K** tautomers are planar. The relatively strong intramolecular hydrogen bond generates a five-membered ring in both the **E** and **K** tautomers. The intramolecular H-bonding is between O-H donor and imine N1 acceptor of the **E** tautomer, but in the case of the **K** tautomer, this interaction is between N-H donor and phenolic O2 acceptor. The hydrogen-bond lengths (N1H5...O2 for the **E** form and O2H5...N1 for the **K** form) are about 1.9 Å.

Therefore, the H-bonding interaction is relatively strong, which cause to a O2-N1 distance of about 2.56 Å in both the tautomers. The calculated D-H5...A hydrogen-bond angles in the **E** and **K** tautomers are 119.91 and 119.37°, respectively.

**TABLE 1 : Selected theoretical structural parameters for the E and K tautomers of TAR and transition state (TS) of E-K tautomerization.**

	<b>E form</b>	<b>K form</b>	<b>TS</b>
Bond length (Å)			
O1-H4	0.9639	0.9646	0.9644
O1-C3	1.3569	1.3567	1.3549
C3-C4	1.3916	1.3981	1.3851
C5-C6	1.4382	1.5009	1.4716
C6-N1	1.3829	1.3498	1.3584
N1-N2	1.2693	1.3011	1.2779
N2-C9	1.3863	1.3546	1.3701
C9-N3	1.3110	1.3155	1.3128
C7-C8	1.3700	1.3690	1.3698
C7-S1	1.7195	1.7240	1.7222
C7-H6	1.0790	1.0788	1.0789
C1-H1	1.0784	1.0789	1.0785
C5-O2	1.3372	1.2429	1.2868
O2-H5	0.9841	1.8901	1.2550
H5-N1	1.9190	1.0362	1.2898
O2-N1	2.5563	2.5626	
Angle (°)			
C1-C2-C3	120.06	120.73	120.51
H5-O2-C5	104.17	85.35	91.59
C1-C6-N1	133.36	130.25	135.81
C5-C6-N1	109.05	108.96	104.23
N1-N2-C9	129.07	125.45	124.64
N2-C9-N3	135.23	133.39	132.84
N2-C9-S1	111.40	113.15	113.41
C9-S1-C7	89.04	88.80	88.78
C7-C8-N3	116.01	116.31	116.15
Dihedral angle (°)			
H4-O1-C3-C2	180.00	180.00	180.00
H5-O2-C5-C6	-0.00	0.00	0.00
C1-C2-C4-C5	0.00	0.00	0.00
O2-C5-C6-N1	0.00	0.01	0.01
C6-N1-N2-C9	-0.02	-0.01	-0.02
N2-C9-S1-C7	180.00	179.99	179.97
S1-C7-C8-N3	-0.01	0.01	0.04
N1-H5-O2-C5	0.00	-0.01	-0.11
C7-C9-C1-C4	179.99	-179.99	179.99
C3-C6-N3-S1	179.99	179.98	-179.98

## Full Paper

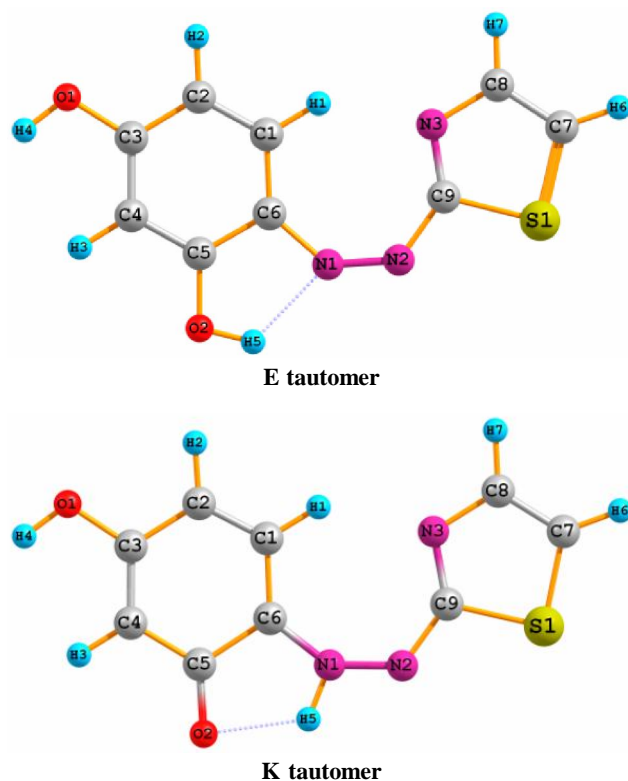


Figure 1 : The B3LYP/6-311+G(d,p) optimized structures of the E and K tautomers of the TAR.

The **E** and **K** tautomers could be converted to each other via an IPT reaction. Some of structural parameters of the **E** form change in the **E**  $\rightarrow$  **K** IPT, the most important of which are: the C2-O1 bond length decreases from 1.3372 in the **E** form to 1.2429 Å in the **K** form, which are corresponding to the phenolic C-O single bond length (1.330 Å) and double C=O bond length (1.210 Å), respectively. Going from the **E** to the **K** tautomer, the C5-O2, C6-N1 and N2-C9 bond lengths decrease, while the C5-C6 and N1-N2 bond lengths increase. Intramolecular hydrogen bond generates a five-membered ring in both conformers. The obtained results are in agreement with the previously reported data for similar compounds<sup>[9,10,14-17]</sup>.

### Mechanism of tautomerization

In continuation, the tautomerization mechanism of the TAR ligand has been theoretically investigated. The obtained transition state for the tautomerization reaction (**TS**) has only one imaginary frequency, confirming its validity.

As seen in Figure 2, the obtained structure for the **TS** is planar (TABLE 1). In the optimized structure of

**TS**, breaking of the O2-H5 bond together with formation of the N1-H5 bond is clear. Going from **E** tautomer to the **TS**, the O2-H5 elongates from 0.9841 to 1.2550 Å, while the N1-H5 distances decreases from 1.9190 to 1.2898 Å.

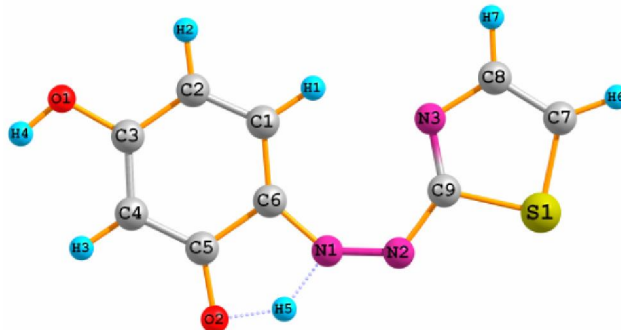


Figure 2 : The B3LYP/6-311+G(d,p) optimized structure of the transition state of the E-K tautomerization.

### Tautomerization energies and solvent effects

Here, the energy contents for the species of the tautomerization were computed in the gas phase and methanol solution. Obviously, the solvent molecules play an important role in chemical reactions. We calculated the solvent effects by handling the PCM model, which is widely used for investigation of the solute-solvent interactions<sup>[20-22]</sup>.

In the gas phase, the **E** tautomer is more stable than the **K** one by 0.74 kcal/mol. However, considering the solvent effects prefers the **K** tautomer in the methanol solution by 1.88 kcal/mol. For the **E**  $\rightarrow$  **K** tautomerization,  $E_a$  in the gas phase and PCM model are 5.62 and 8.05 kcal/mol, respectively.

Solvent effects stabilize all the species. The dipole moment increases during the **E-K** tautomerization, where larger dipole moment leads to larger stabilization effect. The computed dipole moments for the **E**, **K** and **TS** species are 4.17, 4.89 and 3.14 D, respectively. Hence, order of solvation energies is **K** > **E** > **TS**, which results in an exothermic **E**  $\rightarrow$  **K** tautomerization reaction in methanol. Also, because of the lowest dipole moment for the **TS**, the  $E_a$  of the tautomerism reaction increases in the methanol solution compared to the gas phase.

Considering the equilibrium between the **E** and **K** tautomers, the value of the tautomeric equilibrium constant (**K**) is calculated by using

$$K = \exp\left(-\frac{\Delta G}{RT}\right) \quad (1)$$

where  $\Delta G$ ,  $R$  and  $T$  are the Gibbs free energy difference between the **K** and **E** tautomers, the gas constant and temperature, respectively<sup>[21]</sup>. In methanol solution, the  $\Delta G$  is 1.93 kcal/mol, in favor of the **K** tautomer. Hence, using the eq 1, the amount of the **E** form is predicted to be only about 4 %.

### NBO analysis

The NBO analysis is useful method for studying intra- and intermolecular bonding interactions and investigation of charge transfer in chemical compounds<sup>[28]</sup>. During the **E-K** tautomerization, there is a high positive charge on the H5 atom, displaying an IPT between the O2 and N1 atoms. For the **TS**, positive charge on the transferring hydrogen (H5) is higher than the **E** and **K** tautomers.

The amount of stabilization energy of hyper conjugative interactions ( $E(2)$ ), resulting from electron delocalization between donor NBO(i) and acceptor NBO(j) orbitals is a criteria for determining the degree of interaction between electron donor and electron acceptor orbitals. The greater  $E(2)$ , the greater electron transferring tendency from electron donor to electron acceptor, resulting to more electron density delocalization, and consequently leading to more stabilization of the system. The value of  $E(2)$  is calculated by using<sup>[29,30]</sup>

$$E(2) = -q_i \frac{(F_{ij})^2}{\epsilon_j - \epsilon_i} \quad (2)$$

where  $q_i$ ,  $F_{ij}$ ,  $\epsilon_j$  and  $\epsilon_i$  parameters are the donor orbital occupancy, the off-diagonal NBO Fock matrix element, energies of the acceptor and donor orbitals, respectively. These parameters have been obtained from the second-order perturbation theory analysis of Fock matrix in NBO basis. The lower  $\epsilon_j - \epsilon_i$  energy difference results in higher the  $E(2)$  stabilization energy.

Here, the  $E(2)$  energies have been computed for the most stable tautomer, **K** form, the important of which are given in TABLE 2. The strongest electron donation is related to  $n(N2) \rightarrow^* (C6-N1)$  NBO interaction. Electron donation from lone pair of the O2 to the  $\sigma$ -antibonding orbital of the N1-H5 induces high stabilization energy by 7.66 kcal/mol, which increases strength of the intramolecular O2...H5-N1 hydrogen bond.

The distributions and energy levels of the frontier orbitals of the **K** tautomer have been shown in Figure

**TABLE 2: The second-order perturbation theory analysis of Fock matrix in natural bond orbital (NBO) basis for the **K** tautomer.**

Donor NBO (i)	Acceptor NBO	$\epsilon_j - \epsilon_i$ (a.u.)	$F_{ij}$ (a.u.) <sup>b</sup>	$E(2)$ (kcal/mol) <sup>c</sup>
BD (2) C1-C2	BD*(2) C3-C4	0.29	0.068	19.13
BD (2) C3 - C4	BD*(2) C5-O2	0.29	0.083	27.89
BD (2) C6-N1	LP (2) N2	0.15	0.099	37.80
BD (2) C7-C8	BD*(2) N3-C9	0.27	0.054	11.58
BD (2) N3-C9	LP (2) N2	0.12	0.076	28.55
BD (2) N3-C9	BD*(2) C7-C8	0.33	0.076	20.57
LP (2) O1	BD*(2) C3-C4	0.36	0.101	32.68
LP (2) O2	BD*(1) C5-C6	0.68	0.100	18.09
LP (2) N2	BD*(2) C6-N1	0.17	0.107	79.98
LP (2) N2	BD*(2) N3-C9	0.20	0.114	72.07
LP (2) S1	BD*(2) N3-C9	0.24	0.072	26.93
LP (1) N3	BD*(1) S1-C9	0.54	0.083	15.58
LP (2) O2	BD*(1) N9-H20	0.60	0.062	7.66
LP (1) N3	BD*(1) C1-H1	0.85	0.058	4.79

<sup>a</sup>Energy difference between donor (i) and acceptor (j) NBO orbitals; <sup>b</sup>Fock matrix element between i and j NBO orbitals; <sup>c</sup>Energy of hyper conjugative interactions

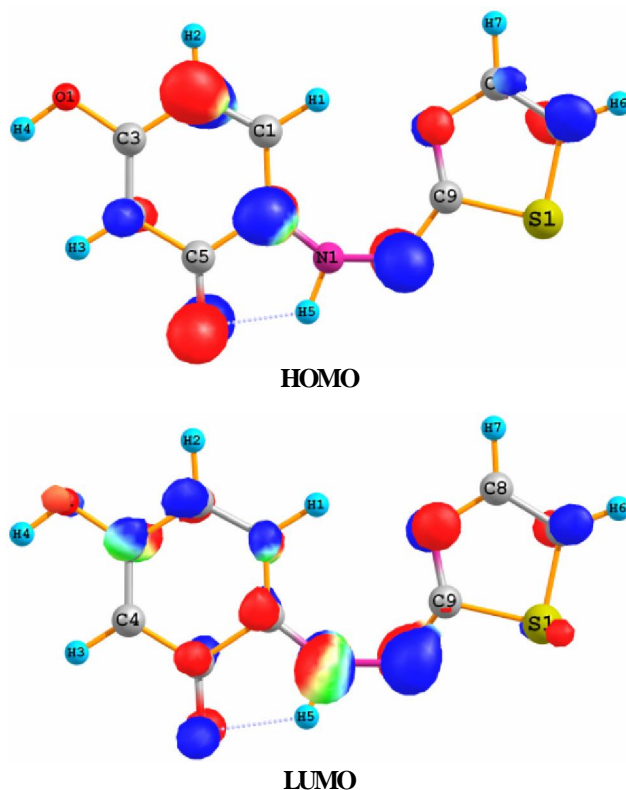


**Figure 3: The HOMO and LUMO frontier orbitals of the **K** tautomer of TAR.**

## Full Paper

3. As seen, the highest occupied molecular orbital (HOMO) is mainly localized on N2, O2, C2 and C6 atoms. While, the lowest-lying unoccupied molecular orbital (LUMO) is mainly localized on the N1 and N2 atoms.

The energy difference between the HOMO and LUMO frontier orbitals is one of the important characteristics of molecules, which has a determining role in such cases as electric properties, electronic spectra and photochemical reactions. For the **K** tautomer, the energy separation between the HOMO and LUMO is 2.47 eV. This large energy gap implies that structure of the **K** tautomer is stable<sup>[31]</sup>.

### CONCLUSIONS

Here, the structural parameters and energetic characters of possible conformers for the TAR as well as its tautomerization mechanism have been theoretically investigated in the gas phase and PCM model. The DFT calculations show that the structures involving all three nitrogens in the same direction are unstable, so that we could not to optimize their structures. We optimize two possible conformers for the TAR, the **E** and **K** tautomers, which were characterized theoretically.

The **E** tautomer is more stable than the **K** tautomer in the gas phase, while solute-solvent interactions prefer the **K** tautomer in methanol. The energy barriers of the **E** → **K** tautomerization in the gas and solution phases are predicted to be 5.62 and 8.05 kcal/mol, respectively. In methanol solution, the  $\Delta G$  between the **E** and **K** tautomers is equal to 1.93 kcal/mol, which shows that amount of the **E** tautomer is about 4 %.

The computed atomic charges support an intramolecular-proton transfer during the tautomerization.

### ACKNOWLEDGEMENT

We gratefully acknowledge financial support from the Islamic Azad University, Mashhad Branch.

### REFERENCES

- [1] F.Karipcin, B.Dede, S.Percin-Ozkorucuklu, E.Kabalcilar; *Dyes PigM.*, **84**, 14 (2010).
- [2] S.Wang, S.Shen, H.Xu; *Dyes Pigm.*, **44**, 195 (2000).
- [3] H.Kocaokutgen, S.Ozkinali; *Dyes Pigm.*, **63**, 83 (2004).
- [4] S.Wu, W.Qian, Z.Xia, Y.Zou, S.Wang, S.Shen; *Chem. Phys.Let.*, **330**, 535 (2000).
- [5] T.Abe, S.Mano, Y.Yamada, A.Tomotake; *J.Imag. Sci.Tech.*, **43**, 339 (1999).
- [6] A.Ikeya, T.Okada; *J.Colloid.Interface.Sci.*, **264**, 496 (2003).
- [7] S.Vicente, N.Manisso, Z.F.Queiroz, E.A.G.Zagatto; *Talanta*, **57**, 475 (2002).
- [8] F.Karipcin, E.Kabalcilar, S.Ilican, Y.Caglar, M.Caglar; *Spectrochim.Acta*, **73**, 174 (2009).
- [9] D.K.Singh, S.Mishra; *Desalination*, **257**, 177 (2010).
- [10] M.Soylak, E.Yilmaz; *J.Hazard.Mater.*, **182**, 704 (2010).
- [11] J.B.Ghasemi, B.Hashemi; *Environ.Mon.Assess.*, (In press).
- [12] K.Ueno, T.Imamura, K.L.Cheng; *CRC Handbook of Organic Analytical Reagents*, CRC Press, 227 (1992).
- [13] E.Bishop; *Indicators*, Pergamon Press, Oxford, 300 (1972).
- [14] R.E.Shepherd; *Coord.Chem.Rev.*, **247**, 159 (2003).
- [15] V.M.Ivanov, O.V.Kuznetsova; *J.Anal.Chem.*, **55**, 899 (2000).
- [16] R.W.Stanley, G.E.Cheney; *Talanta*, **13**, 1619 (1966).
- [17] F.Karipcin, E.Kabalcilar, S.Ilican, Y.Caglar, M.Caglar; *Spectrochim.ActaPart A*, **73**, 174 (2009).
- [18] A.Jeziarska-Mazzarello, R.Vuilleumier, J.J.Panek, G.Ciccotti; *J.Phys.Chem.B*, **114**, 242 (2010).
- [19] R.D.Bach, C.Canepa, M.N.Glukhovtsev; *J.Am. Chem.Soc.*, **121**, 6542 (1999).
- [20] S.Chowdhury, F.Himo, N.Russo, E.Sicilia; *J.Am. Chem.Soc.*, **132**, 4178 (2010).
- [21] S.A.Beyramabadi, H.Eshtiagh-Hosseini, M.R.Housaindokht, A.Morsali; *Organometallics*, **27**, 72 (2008).
- [22] S.A.Beyramabadi, H.Eshtiagh-Hosseini, M.R.Housaindokht, A.Morsali; *J.Mol.Struct: THEOCHEM*, **903**, 108 (2009).
- [23] H.Eshtiagh-Hosseini, M.R.Housaindokht, S.A.Beyramabadi, S.Beheshti, A.A.Esmaeili, M.Javan-Khoshkholgh, A.Morsali; *Spectrochim. ActaPartA*, **71**, 1341 (2008).
- [24] S.A.Siddiquia, R.Srivastavab, S.Jainc, N.Misrab; *Phys.Chem.:An IndianJ.*, **5**, (2010).

- [25] M.J.Frisch, et al.; Gaussian 98, Revision A.7, Gaussian, Inc.: Pittsburgh PA, (1998).
- [26] C.Lee, W.Yang, R.G.Parr; Phys.Rev.B, **37**, 785 (1988).
- [27] J.Tomasi, R.Cammi; J.Comput.Chem., **16**, 1449 (1995).
- [28] M.Snehalatha, C.Ravikumar, I.Hubert Joe, N.Sekar, V.S.Jayakumar; Spectrochim.ActaA, **72**, 654 (2009).
- [29] D.W.Schwenke, D.G.Truhlar; J.Chem.Phys., **82**, 2418 (1985).
- [30] M.Gutowski, G.Chalasinski; J.Chem.Phys., **98**, 4728 (1993).
- [31] N.Tezer, N.Karakus; J.Mol.Model, **15**, 223 (2009).